

# $^{12}\text{C}+^{12}\text{C}$ and $^{16}\text{O}+^8\text{Be}$ decay of $^{24}\text{Mg}$ states populated in the $^{12}\text{C}(^{20}\text{Ne}, ^{24}\text{Mg}^*)^8\text{Be}$ reaction

M. Freer, J. T. Murgatroyd, and S. M. Singer

*School of Physics and Astronomy, University of Birmingham, Edgbaston, Birmingham B15 2TT, United Kingdom*

N. Curtis\*

*School of Physics and Chemistry, University of Surrey, Surrey GU2 7XH, United Kingdom*D. J. Henderson, D. J. Hofman,<sup>†</sup> and A. H. Wuosmaa*Physics Division, Argonne National Laboratory, 9700 South Cass Avenue, Argonne, Illinois 60439*

(Received 30 October 2000; published 20 February 2001)

The  $^{12}\text{C}+^{12}\text{C}$  and  $^8\text{Be}+^{16}\text{O}$  decay of  $^{24}\text{Mg}$  states populated in the  $^{12}\text{C}(^{20}\text{Ne}, ^{24}\text{Mg}^*)$  reaction has been studied at beam energies of 160 and 110 MeV. Evidence for excited states, which decay by  $^{12}\text{C}$  and  $^8\text{Be}$  emission, is observed for the excitation energy range 22 to 33 MeV. Angular correlation analysis shows that the spins of these states lie in the range of 6 to  $12\hbar$ . These measurements further indicate that the breakup states possess a 4p-4h structure.

DOI: 10.1103/PhysRevC.63.034317

PACS number(s): 25.70.Ef, 27.30.+t

## I. INTRODUCTION

The study of the spectroscopy of nuclei at excitation energies in excess of 10 to 20 MeV is a considerable challenge. Typically both backgrounds and level densities mask the states of interest. Moreover, for states populated as resonances with spins greater than a few units, populated in inelastic scattering or transfer reactions, the angular distributions are often featureless, prohibiting the extraction of angular momentum information. Breakup reactions, however, may be used to successfully combat these difficulties [1]. In such measurements, the binary decay of the excited states is observed by recording the two decay products in coincidence, and the excitation energy of the parent system may then be reconstructed in a relatively background free environment. The measurement of the emission angle distributions in the center-of-mass frame of the decaying nucleus may also be used to provide a relatively model independent determination of their spins [2,3].

This experimental technique has been used successfully to study the  $^{12}\text{C}+^{12}\text{C}$  decay properties of the nucleus  $^{24}\text{Mg}$ . In a region of excitation energy, 20 to 40 MeV, where the density of states is considerable, the decay of specific states into two  $^{12}\text{C}$  nuclei is observed, and a series of measurements have produced detailed spin information [4–6]. The trend in the energy-spin systematics of these states follows a rotational  $J(J+1)$  trajectory with a moment of inertia which indicates that the decay is from a highly deformed  $^{24}\text{Mg}$  excited configuration, reminiscent of the resonances observed in  $^{12}\text{C}+^{12}\text{C}$  scattering measurements [7]. It is possible to interpret these data in terms of the decay of a shape

isomeric configuration, associated with a secondary minimum in the deformed potential. Such a minimum would result from shell structure in the single-particle level scheme of the deformed potential, as observed in systems with superdeformed bands and fission isomers. Shape isomeric structures are in fact predicted by a variety of nuclear models, for example Nilsson-Strutinsky [8], Hartree-Fock [9], and also alpha cluster model [10] calculations.

These models, however, predict not only one shape isomer but several, many of which have structural characteristics which would allow the decay into two  $^{12}\text{C}$  nuclei. Assuming that the breakup states are associated with a unique isomer it is therefore not clear which one. The mechanism by which the states are populated may offer an answer. It has been observed [11] that such states are most strongly populated via the  $^{12}\text{C}(^{20}\text{Ne}, ^{24}\text{Mg})$  reaction [12] when compared with, for example, inelastic excitation [4] or via the more complex  $^{12}\text{C}(^{16}\text{O}, ^{24}\text{Mg})$  reaction [6]. This comparison would indicate that the states in  $^{24}\text{Mg}$  with large  $^{12}\text{C}+^{12}\text{C}$  decay branches possess a close link with a 4p-4h configuration built on a  $^{20}\text{Ne}_{gs}$  core. No spins, however, have been measured for the states populated via the  $\alpha$ -transfer reaction and thus connection with the breakup states observed in other reactions cannot be assured.

In this paper we present a study of the  $^{12}\text{C}(^{20}\text{Ne}, ^{12}\text{C}^{12}\text{C})^8\text{Be}$  and  $^{12}\text{C}(^{20}\text{Ne}, ^8\text{Be}^{16}\text{O})^8\text{Be}$  reactions aimed at determining the excitation energies and spins of the states previously observed in previous work [12,13].

## II. EXPERIMENTAL DETAILS

The  $^{12}\text{C}(^{20}\text{Ne}, ^{12}\text{C}^{12}\text{C})^8\text{Be}$  and  $^{12}\text{C}(^{20}\text{Ne}, ^8\text{Be}^{16}\text{O})^8\text{Be}$  reactions were studied at the Argonne National Laboratory ATLAS linac facility.  $^{20}\text{Ne}$  beams of energies 160 and 110 MeV, with intensities of  $\sim 50$  enA, were incident on  $50\ \mu\text{g}\ \text{cm}^{-2}$  natural carbon targets. The integrated beam exposures for the two energies were 15.1 and 2.8 mC, respectively.

\*Present address: School of Physics and Astronomy, University of Birmingham, Edgbaston, Birmingham B15 2TT, U.K.

<sup>†</sup>Present address: Physics Department, University of Illinois at Chicago, 845 West Taylor Street, Chicago, IL 60607.

The  $^{16}\text{O}$ ,  $^{12}\text{C}$ , and  $^8\text{Be}$  decay products were detected in two gas-silicon hybrid telescopes. The gas ionization chambers, operated at pressure of 50 Torr with 5  $\mu\text{m}$  thick Mylar windows, and possessing a 5 cm active depth, provided the  $\Delta E$  signal. The silicon elements of the telescopes were 5 cm by 5 cm, 16 element, position-sensitive strip-detectors. These detectors provided a measurement of the full energy of the incident ions and their position with resolutions of 300 keV and 0.25 mm, respectively. The segmentation of the silicon detectors also allowed the detection of the two  $\alpha$ -particles from the decay of the  $^8\text{Be}$  nuclei within a single telescope. Further details of the performance of these detectors is given in Ref. [14]. The silicon elements of the telescopes were placed 18.0 cm from the target and symmetrically about the beam axis at an angle of  $18.0^\circ$ . The uncertainty in the angles of the detectors is  $0.1^\circ$  which leads to a systematic uncertainty in the reconstructed excitation energies of  $\sim 200$  keV.

The performance of the detectors was calibrated using  $\alpha$ -source measurements and elastic scattering of 80 MeV  $^{12}\text{C}$  nuclei from  $^{12}\text{C}$ ,  $^{27}\text{Al}$ , and  $^{197}\text{Au}$  targets.

### III. DATA ANALYSIS AND RESULTS

By plotting the measured gas signal against the energy deposited in the strip detectors it was possible to identify incident ions with charges  $Z=6$  and  $Z=8$  (the detectors do not provide explicit mass resolution). Identification of  $^8\text{Be}$  decays was made by reconstructing the  $^8\text{Be}$  excitation energy spectrum for all events in which particles entered two strips within a single detector. The reconstructed peak at an energy of 92 keV was then used as a unique signature for the detection of  $^8\text{Be}$  nuclei.

Following the identification of the decay products, sum energy spectra were calculated for  $^{12}\text{C}+^{12}\text{C}$  and  $^8\text{Be}+^{16}\text{O}$  coincidences,

$$E_{tot} = E_1 + E_2 + E_{recoil}, \quad (1)$$

where  $E_1$  and  $E_2$  are the energies of the detected fragments and  $E_{recoil}$  is the energy of the unobserved recoil, reconstructed from the momenta of the two detected breakup products.  $E_{tot}$  is related to the reaction  $Q$  value via  $Q = E_{tot} - E_{beam}$ . The associated sum energy spectra are shown in Fig. 1. The peaks in these spectra may be then used to isolate the various final states of the  $^{12}\text{C}$  and  $^{16}\text{O}$  nuclei. For example, in Fig. 1(a) a peak is observed at  $E_{tot} = 147.8$  MeV ( $Q = -12.2$  MeV) corresponding to the final state in the  $^{12}\text{C}(^{20}\text{Ne}, ^{16}\text{O}^8\text{Be})^8\text{Be}$  reaction where all nuclei are left in their ground states ( $Q = -12.19$  MeV). The  $2^+$  excitation of the  $^8\text{Be}$  recoil may also be observed in this spectrum. Similarly, in Fig. 1(b) there is a peak at  $E_{tot} = 147.8$  MeV ( $Q = -12.2$  MeV) corresponding to all of the final state nuclei in the  $^{12}\text{C}(^{20}\text{Ne}, ^{12}\text{C}^{12}\text{C})^8\text{Be}$  reaction being formed in their ground states ( $Q = -11.98$  MeV). Monte Carlo simulations of the reaction and detection processes, including the experimental resolutions, indicate that the  $E_{tot}$  resolution should be 1.3 MeV [full width at half maximum (FWHM)], in reasonable agreement with the experimental measurements.

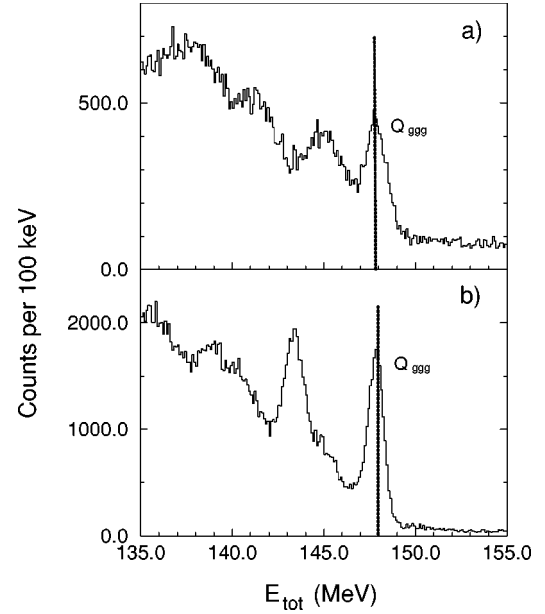


FIG. 1. Total energy spectra for the (a)  $^{12}\text{C}(^{20}\text{Ne}, ^{16}\text{O}^8\text{Be})^8\text{Be}$  and (b)  $^{12}\text{C}(^{20}\text{Ne}, ^{12}\text{C}^{12}\text{C})^8\text{Be}$  reactions at  $E_{beam} = 160$  MeV. The vertical dotted line indicates the expected sum energy for a final state in which all particles are produced in their ground states.

By gating on the peaks in Fig. 1 labeled  $Q_{ggg}$ , events in which all final state particles were produced in their ( $J=0$ ) ground states could be selected. The  $^{24}\text{Mg}$  excitation-energy spectrum was then calculated from the measured emission energies and angles of the detected fragments. Figure 2 shows the reconstructed excitation energies for the two decay channels at the beam energies of 160 and 110 MeV. The lines in these spectra are the results of Monte Carlo simulations of the experimental detection efficiencies. These calculations simulate the response of the detectors in terms of the

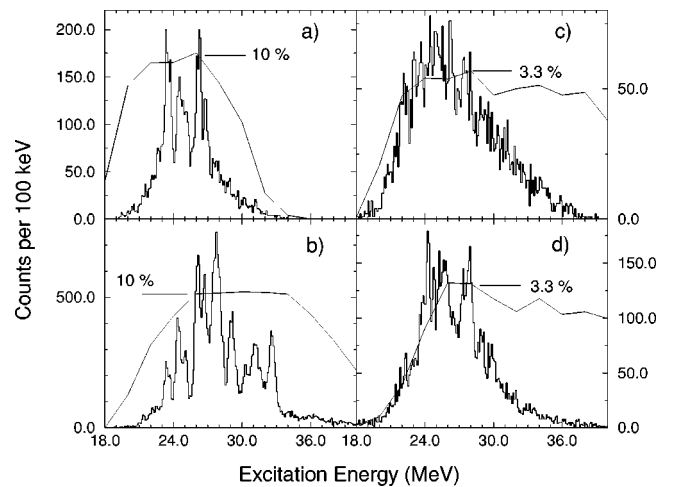


FIG. 2. Excitation energy spectra for the (a)  $^{12}\text{C}+^{12}\text{C}$  decay channel at  $E_{beam} = 110$  MeV, (b)  $^{12}\text{C}+^{12}\text{C}$  decay channel at  $E_{beam} = 160$  MeV, (c)  $^{16}\text{O}+^8\text{Be}$  decay channel at  $E_{beam} = 110$  MeV, and (d)  $^{16}\text{O}+^8\text{Be}$  decay channel at  $E_{beam} = 160$  MeV. The line in each plot is the calculated detection efficiency for each reaction.

energy and angular acceptances and also attempt to generate reaction products with realistic energy and angular distributions. The reaction process is simulated by assuming that the initial  $^{12}\text{C}(^{20}\text{Ne}, ^{24}\text{Mg}^*)^8\text{Be}$  reaction proceeds via  $\alpha$ -transfer and may be reproduced by a simple exponential form. The decay process is, on the other hand, assumed to be isotropic. As the experiment was sensitive to  $^{24}\text{Mg}$  emission angles close to  $0^\circ$  then the detection efficiency depends only weakly on the exponential falloff factor used in the simulations. These approximations lead to an uncertainty in the absolute detection efficiency, but do provide a more accurate determination of the relative detection efficiencies for the two channels and, most importantly, they provide an indication of how the efficiency varies with the changing  $^{24}\text{Mg}$  excitation energy. Figures 2(a) and 2(b) show the reconstructed excitation energy spectra for the  $^{12}\text{C}+^{12}\text{C}$  decay channel for the 110 MeV and 160 MeV beam energies respectively. Similarly, Figs. 2(c) and 2(d) show the excitation energy spectra for the  $^8\text{Be}+^{16}\text{O}$  decays. It is immediately apparent that the structure in the  $^{12}\text{C}+^{12}\text{C}$  decay channel is much more pronounced than for the  $^8\text{Be}+^{16}\text{O}$  decays, due in part to the symmetry of the  $^{12}\text{C}+^{12}\text{C}$  decay process, which samples only states with even spin, and natural parity. On the other hand, both even and odd spin states, but still of natural parity, can feed the asymmetric decay channel, and hence the density of states in these excitation energy spectra is larger.

The peaks in the  $^{12}\text{C}+^{12}\text{C}$  spectra for the two beam energies are correlated and agree within 100 keV, suggesting that the same set of states are populated at the two beam energies. There is less evidence for correlated structures in the two  $^8\text{Be}+^{16}\text{O}$  decay spectra. However, there would appear to be strong evidence for isolated states in this decay channel for the higher energy data [Fig. 2(d)]. The  $E_{tot}$  spectra in Fig. 1 indicates that there is a larger background contribution to this breakup channel, which, in part, may account for the slightly poorer quality of the excitation energy spectra.

The peak detection efficiencies for the two decay channels differ by a factor of 3, indicating that the decay probabilities for the two channels are of a similar magnitude. There is at least one significant difference between the spectra for the two decay channels. Particularly in the 160 MeV data, the structure in the  $^8\text{Be}+^{16}\text{O}$  decay channel is much more strongly damped than in the mass symmetric decay channel above 30 MeV. This contrasting behavior may point to a significant difference between the states feeding the two decay channels.

Finally, the Monte Carlo simulations suggest that the experimental excitation energy resolution is 400 keV, thus many of the widths are dominated by the experimental resolution and the natural widths are not observed for the majority of the states.

### A. Angular correlations

The determination of the full ground state kinematics permits the reconstruction of the emission angles of the decay products in both the  $^{12}\text{C}+^{20}\text{Ne}$ , and  $^{24}\text{Mg}^*$  center-of-mass frames, allowing the spins of the decaying states to be de-

duced via an analysis of the correlation between the emission angles in the two frames. This experimental technique is described in detail in Ref. [15] and references therein. Briefly, the excitation and decay processes can be described in terms of two sets of spherical-polar coordinates;  $(\theta^*, \phi^*)$  for the primary reaction, and  $(\psi, \chi)$  for the decay process. Here,  $\theta^*$  is the scattering angle and  $\psi$  is the decay angle, with both measured with respect to the beam axis.

Typically, for reactions involving spin zero initial and final state particles the number of reaction amplitudes are small and the correlations observed between the two angles  $\theta^*$  and  $\psi$  take the form of a sloping ridge pattern. The periodicity of the ridges is described by a Legendre polynomial of order of the spin of the decaying state, i.e.,  $P_J(\cos \psi)$ . As the dominant orbital angular momenta in the reaction are those corresponding to grazing trajectories, the gradient of the ridges is typically given by the ratio of the exit channel grazing angular momentum to the spin of the state populated

$$\frac{\Delta \theta^*}{\Delta \psi} = \frac{J}{l_f} = \frac{J}{l_i - J}, \quad (2)$$

where  $l_i$  and  $l_f$  are the initial and final state grazing angular momenta. If the ‘‘stretched’’ configuration dominates, which is typically the case for such reactions (see [15] and references therein), then the entrance and exit channel angular momenta can be related via the expression  $l_f = l_i - J$ .

The angular correlations therefore provide two signatures of the spin of the decaying  $^{24}\text{Mg}$  state. The periodicity yields a value for  $J$ , which should correlate with that extracted from the ridge gradient, assuming  $l_i$  is known. In addition, the value of  $J$  extracted from the periodicity should provide a consistent value of  $l_i$  for all of the correlations. Figures 3–6 show the projection of the two dimensional  $\theta^* - \psi$  correlations, along the ridge locii, onto the  $\theta^* = 0$ ,  $\psi$  axis. The angle of projection is selected that maximizes the peak to valley ratio. In this way the periodicity of the correlations can be compared with the functions  $P_J(\cos \psi)$  in order to extract the spin  $J$  of each states. The results of this analysis, including the values of  $l_i$  deduced from the projection angle, are given in Tables I–III.

### $^{12}\text{C}+^{12}\text{C}$ angular distributions

For the  $^{12}\text{C}+^{12}\text{C}$  decay channel the peak at  $\sim 23.5$  MeV in the two data sets appears to have a spin of 8 [Fig. 3(a) and Fig. 5(b)], and the shape of the peaks at the two energies suggests that actually there may be two overlapping states. Similarly, at 24.5 (24.6 MeV in the 110 MeV data) and 25.1 MeV the angular correlation analysis for both beam energies [Figs. 3(b), 3(c), 5(c), and 5(d)] suggests that the states are dominated by  $J=8$ . The next peak in this decay channel is at 26.2 MeV (26.3 in the 110 MeV data), and at both energies the correlation analysis indicates  $J=10$  [Figs. 3(d) and 5(e)]. Again, there is good agreement between the two measurements with  $J=10$  states observed at 26.8 MeV (26.9 in the 110 MeV data) and 27.8 MeV.

Analysis suggests that the peak at 29.1 MeV has contributions from spins  $J=10$  and 12, as gates on the low [Fig.

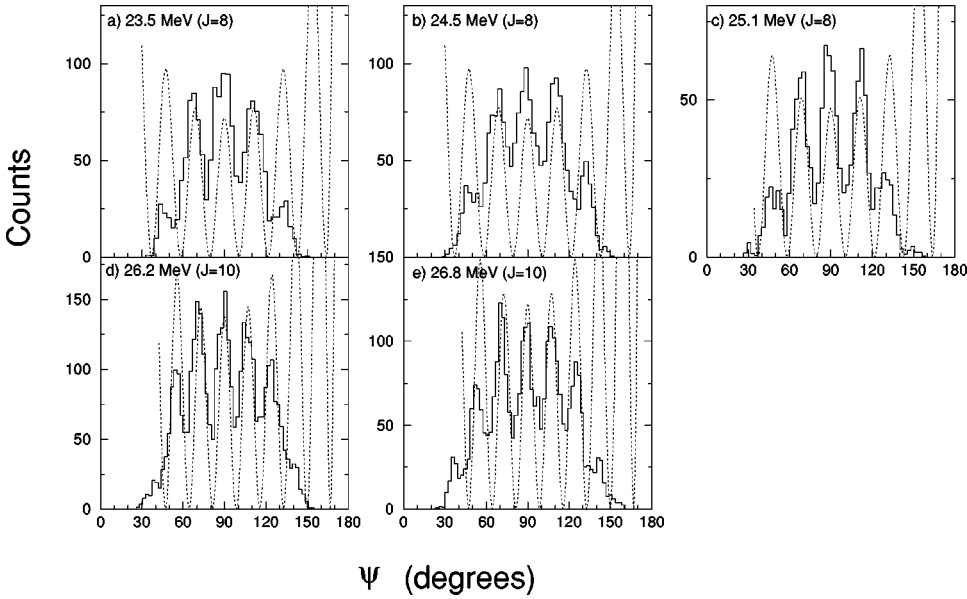


FIG. 3. Projected angular correlations for the states observed in the  $^{12}\text{C}+^{12}\text{C}$  decay channel at  $E_{beam}=160$  MeV, for excitation energies of 20 to 27 MeV. The solid line in each case corresponds to a  $|P_J|^2$  function, where  $J$  is the spin assigned to the state.

4(b)] and high excitation energy [Fig. 4(c)] sides indicates differing dominant spins. The states at  $E_x=30.3$  and 31.2 MeV appear only in the  $E_{beam}=160$  MeV data and the correlations indicate that both possess  $J=12$ . Finally, the 32.7 MeV state observed at  $E_{beam}=160$  MeV has a correlation that strongly suggests  $J=10$  [Fig. 4(f)], however, the value of  $l_i$  is some 3 units less than the mean value at this beam energy. This might indicate an incorrect spin assignment. The results of the above analysis are summarized in Tables I and II.

#### $^8\text{Be}+^{16}\text{O}$ angular distributions

Unfortunately, the analysis of the  $^8\text{Be}+^{16}\text{O}$  decay channel does not yield such unambiguous results. The number of peaks in Figs. 2(c) and 2(d) which show strong correlation patterns is significantly less than for the symmetric decay channel. This can be explained by the presence of the expected larger number of different spin states that can decay to this final state. For the 110 MeV data no strong oscillatory

correlations are observed. However, the 160 MeV data appears to be slightly clearer, which is also indicated by the more structured excitation energy spectrum. As with the  $^{12}\text{C}$  decay channel several of the peaks appear to possess contributions from several states. There is some indication of a peak at 23.0 MeV and a gate to low excitation energy indicates  $J=8$  [Fig. 6(a)] while a gate on the high energy side suggests  $J=6$  [Fig. 6(b)]. There also appears to be a broad structure at 23.8 MeV, which appears to only contain  $J=8$  contributions [Figs. 6(c) and 6(d)], and this would coincide with the  $J=8$  state at approximately the same energy observed in the spectra in Figs. 2(a) and 2(b) (23.5 MeV). There is also a  $J=10$  state at 27.9 MeV which could correspond to the state at 27.8 MeV in the  $^{12}\text{C}$  decay channel with the same spin.

On the whole there is good agreement in the reconstructed  $l_i$  values for the above analysis of the two decay channels. At  $E_{beam}=160$  MeV  $\bar{l}_i=30.3\hbar$  and  $30.4\hbar$  for the  $^{12}\text{C}$  and  $^8\text{Be}$  decay channels, respectively, and  $\bar{l}_i=22.7\hbar$  for the  $^{12}\text{C}$  decay channel at  $E_{beam}=110$  MeV. The observed change in  $l_i$

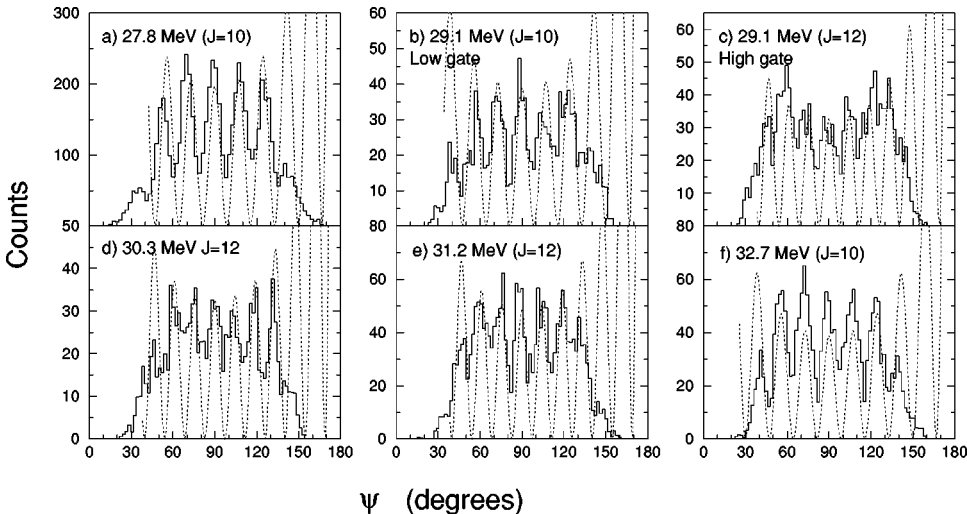


FIG. 4. Projected angular correlations for the states observed in the  $^{12}\text{C}+^{12}\text{C}$  decay channel at  $E_{beam}=160$  MeV, for excitation energies of 27 to 33 MeV. The solid line in each case corresponds to a  $|P_J|^2$  function, where  $J$  is the spin assigned to the state.

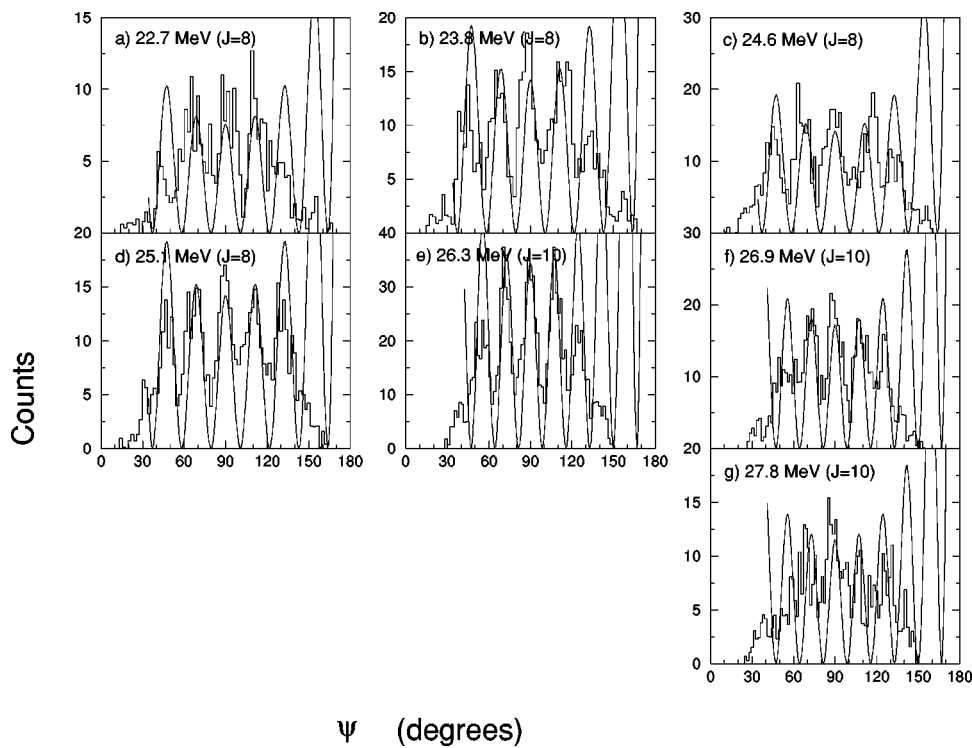


FIG. 5. Projected angular correlations for the states observed in the  $^{12}\text{C}+^{12}\text{C}$  decay channel at  $E_{beam}=110$  MeV. The solid line in each case corresponds to a  $|P_J|^2$  function, where  $J$  is the spin assigned to the state.

with the beam energy is consistent with the scaling deduced from the change in center-of-mass energy.

#### IV. DISCUSSION

The present study represents an advance over the previous measurements of the  $^{12}\text{C}(^{20}\text{Ne},^{12}\text{C}^{12}\text{C})$  reaction, as here we present comprehensive spin assignments. This permits, for

the first time, a detailed comparison to be made with  $^{12}\text{C}+^{12}\text{C}$  breakup states observed in other reactions.

The present measurements may be compared with those already reported for the  $^{12}\text{C}(^{20}\text{Ne},^{12}\text{C}^{12}\text{C})$  [12,16,17] and  $^{12}\text{C}(^{20}\text{Ne},^8\text{Be}^{16}\text{O})$  [13] reactions. First, the spectrum of  $^{24}\text{Mg}^{12}\text{C}+^{12}\text{C}$  breakup states observed in the present 160 MeV measurement is almost identical to that reported for the study with the same reaction and beam energy in Refs.

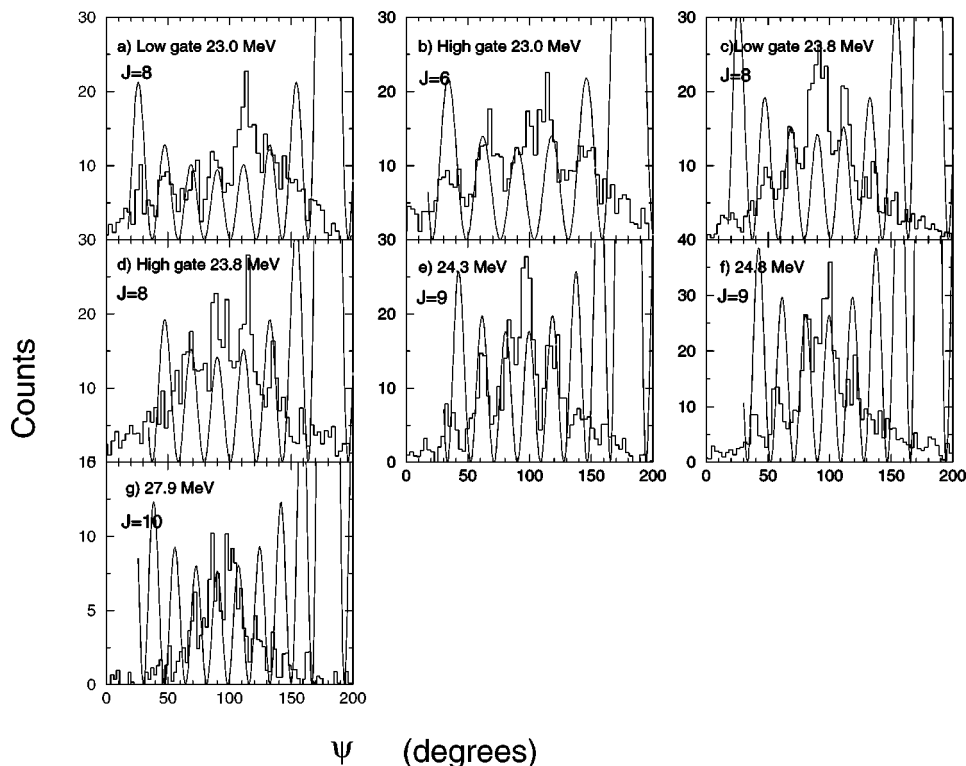


FIG. 6. Projected angular correlations for the states observed in the  $^{16}\text{O}+^8\text{Be}$  decay channel at  $E_{beam}=160$  MeV. The solid line in each case corresponds to a  $|P_J|^2$  function, where  $J$  is the spin assigned to the state.

TABLE I. Properties of states observed in the  $^{12}\text{C}+^{12}\text{C}$  decay channel for  $E_{beam}=160$  MeV. In the instance that the correlation analysis indicates that a peak may be associated with multiple spins both are indicated, but not a value of  $l_i$ .  $\bar{l}_i=30.3\hbar$ .

$E_x$ (MeV)	$J$	$l_i$
23.4	8	30.9( $\pm 1.5$ )
24.5	8,6	
25.1	8	27.6( $\pm 1.5$ )
26.2	10	30.3( $\pm 1.0$ )
26.8	10	30.6( $\pm 1.0$ )
27.8	10	31.4( $\pm 1.0$ )
29.1	10,12	
30.3	12	32.4( $\pm 0.8$ )
31.2	12	32.1( $\pm 0.8$ )
32.7	10	26.8( $\pm 0.8$ )

[12,17]. The present measured excitation energies are, however, 300 keV systematically lower. This discrepancy is consistent with the 200 keV systematic uncertainty in the present measurement and the uncertainty of the same order present in the earlier measurements. Furthermore, the spectrum of states observed in the  $^{16}\text{O}+^8\text{Be}$  decay channel is very similar to that reported in [13] (including the reported excitation energies), in the study of the  $^{12}\text{C}(^{20}\text{Ne},^8\text{Be}^{16}\text{O})$  reaction at  $E_{beam}=160$  MeV. In fact, in this latter study a  $9^-$  state was observed at an energy of 24.43 MeV, which would correspond to the measured  $J=9$  for the 24.3 MeV state.

Detailed spin measurements have also been reported for the study of the  $^{12}\text{C}(^{16}\text{O},^{12}\text{C}^{12}\text{C})$  and  $^{12}\text{C}(^{16}\text{O},^8\text{Be}^{16}\text{O})$  reactions [6]. These are compared, for the  $^{12}\text{C}+^{12}\text{C}$  decay channel, with the present measurements in Table IV. Apart from a small discrepancy in energy ( $\sim 200$  keV), there appears to be good agreement between the energies and spins of the states for the excitation energy range of 26.4 to 29.2 MeV. This agreement is not so good above and below these limits since the strength of the  $^{12}\text{C}(^{16}\text{O},^{12}\text{C}^{12}\text{C})$  reaction seems to be attenuated at lower energies while the opposite is true for the  $^{12}\text{C}(^{20}\text{Ne},^{12}\text{C}^{12}\text{C})$  data. However, as noted in [12,17] if angular momentum matching is important in the present  $\alpha$ -transfer reaction then the matching is best for  $J$  values of 8 to 10, with a calculated suppression by one

TABLE II. Properties of states observed in the  $^{12}\text{C}+^{12}\text{C}$  decay channel for  $E_{beam}=110$  MeV. In the instance that the correlation analysis indicates that a peak may be associated with multiple spins both are indicated, but not a value of  $l_i$ .  $\bar{l}_i=22.7\hbar$ .

$E_x$ (MeV)	$J$	$l_i$
22.7	6,8	
23.5	8	24.0( $\pm 1.0$ )
24.6	8	22.0( $\pm 1.0$ )
25.1	8	22.1( $\pm 1.0$ )
26.3	10	23.2( $\pm 1.0$ )
26.9	10	23.9( $\pm 1.0$ )
27.8	10	22.8( $\pm 1.0$ )

TABLE III. Properties of states observed in the  $^{16}\text{O}+^8\text{Be}$  decay channel for  $E_{beam}=160$  MeV. The more tentative spin assignments are shown in brackets.  $\bar{l}_i=30.4\hbar$ .

$E_x$ (MeV)	$J$	$l_i$
22.4	(8)	
23.0	6,8	
23.8	8	28.2( $\pm 1.5$ )
24.3	9	32.8( $\pm 1.5$ )
24.8	9	30.3( $\pm 1.5$ )
(25.3)		
25.8	(9/10)	
27.4		
27.9	(10)	
29.0		
29.9		

order of magnitude for  $J=6$  and 12. Similar calculations using Brink's prescription [18] suggests that the reduction of the beam energy to 110 MeV should enhance the  $J=8$  states with  $J=6$  suppressed by a factor of 2 and  $J=4$  by 20. The dominance of spins of 8 and 10 in the 160 MeV data, and the shift towards states with spins of 8 for the 110 MeV beam energy is thus in agreement with these matching calculations. On the other hand, the  $^{12}\text{C}(^{16}\text{O},^{12}\text{C}^{12}\text{C})$  reaction is likely to

TABLE IV. A comparison between the excitation energies and spins of  $^{24}\text{Mg}$  states observed in the  $^{12}\text{C}+^{12}\text{C}$  decay channel in the present measurement and those in Ref. [6]. Where states are observed at  $E_{beam}=160$  and 110 MeV the average value of  $E_x$  is used.

$^{12}\text{C}(^{16}\text{O},^{24}\text{Mg})$		$^{12}\text{C}(^{20}\text{Ne},^{24}\text{Mg})$	
$E_x$ (MeV)	$J$	$E_x$ (MeV)	$J$
20.9	(6)		
21.7	(6)		
22.7	(4/6)	22.7	6,8
23.4	(4)	23.4	8
23.8	(6)		
24.2	(8)	24.5	8
25.0	8	25.1	8
25.9	(10)		
26.4	(10)	26.2	10
27.0	10	26.8	10
28.0	10	27.8	10
28.4	10		
29.2	12	29.1	10/12
30.0	10		
		30.3	12
		31.2	12
31.9	12		
(32.5)	(12)		
		32.7	10
33.2	12		
35.6	14		
36.7	(14)		

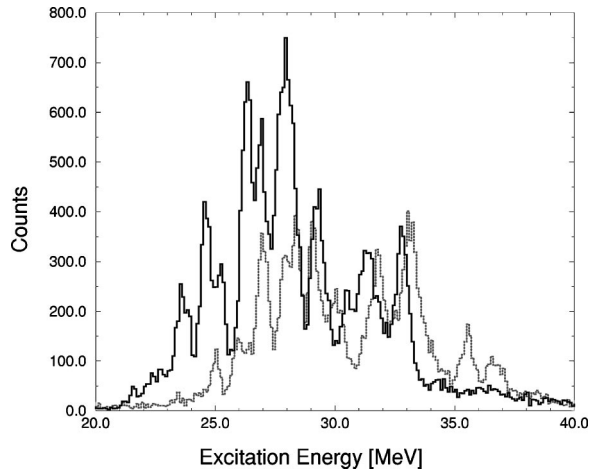


FIG. 7. A comparison between the 160 MeV  $^{12}\text{C}+^{12}\text{C}$  excitation energy spectrum from the  $^{12}\text{C}+^{20}\text{Ne}$  entrance channel (solid histogram) and the  $^{12}\text{C}+^{12}\text{C}$  breakup spectrum (dotted histogram) from the  $^{12}\text{C}(^{16}\text{O}, ^{12}\text{C}^{12}\text{C})$  ( $E_{beam} = 115$  MeV) reaction. The excitation energy scale for the former has been adjusted by +200 keV.

be more complex, perhaps even proceeding through the  $^{28}\text{Si}$  compound system as proposed in [6]. This analysis would suggest that the difference between the two reactions at the extremes of the excitation energy range arises due to the weaker population of states with spin greater or less than 8 and 10. Figure 7 shows the two spectra for the reactions  $^{12}\text{C}(^{16}\text{O}, ^{12}\text{C}^{12}\text{C})$  ( $E_{beam} = 115$  MeV) and  $^{12}\text{C}(^{20}\text{Ne}, ^{12}\text{C}^{12}\text{C})$  ( $E_{beam} = 160$  MeV) overlaid (the latter spectrum has been shifted by +200 keV). Again, the observed agreement suggests that the two reactions are in fact probing the same states in  $^{24}\text{Mg}$ .

Table V presents a similar comparison for the  $^{16}\text{O}+^8\text{Be}$  decay channels. However, due to the increased complexity of the spectra and the greater uncertainty in the spin assignments, this decay channel does not bear the level of scrutiny applied above to the symmetric decay channel. However, there appear to be qualitative similarities in the states populated in the two reactions, in that the spins of the states lie in the same region. This may also indicate that the two reactions probe the same structures in the  $^{24}\text{Mg}$  nucleus.

Figure 8 shows a comparison of the energy-spin systematics of the resonances observed in the reactions (a)  $^{12}\text{C}(^{20}\text{Ne}, ^{12}\text{C}^{12}\text{C})$ , (b)  $^{12}\text{C}(^{16}\text{O}, ^{12}\text{C}^{12}\text{C})$ , and (c)  $^{12}\text{C}+^{12}\text{C}$ . A linear fit to these systematics is shown in Table VI. The agreement between the fit parameters for the  $^{12}\text{C}(^{20}\text{Ne}, ^{12}\text{C}^{12}\text{C})$  and  $^{12}\text{C}(^{16}\text{O}, ^{12}\text{C}^{12}\text{C})$  reactions is excellent, strengthening the link between the observed states. There is less agreement with the  $^{12}\text{C}+^{12}\text{C}$  scattering resonance data, where the gradient is steeper. This may suggest that only a subset of the scattering resonances is observed in the breakup reactions, and that perhaps the scattering resonances may be linked with more than one rotational structure.

Earlier Murgatroyd *et al.* [16] had suggested that from a measurement of the  $^{12}\text{C}(^{20}\text{Ne}, ^{12}\text{C}^{12}\text{C})$  reaction at  $E_{beam} = 300$  MeV, where no further states were observed beyond those at 31.2 and 32.7 MeV seen in the present measurement, that there was a termination of a rotational band linked with

TABLE V. A comparison between the excitation energies and spins of  $^{24}\text{Mg}$  states observed in the  $^{16}\text{O}+^8\text{Be}$  decay channel in the present measurement and those in Ref. [6].

$^{12}\text{C}(^{16}\text{O}, ^{24}\text{Mg})$		$^{12}\text{C}(^{20}\text{Ne}, ^{24}\text{Mg})$	
$E_x$ (MeV)	$J$	$E_x$ (MeV)	$J$
20.8			
22.1	(6,8)	22.4	(8)
23.1	(6)	23.0	6,8
23.4	(8)		
		23.8	(8)
		24.3	(9)
24.8	(9,11)	24.8	(9)
		(25.3)	
25.7	(9,11)	25.8	(9/10)
26.7			
27.3	(9,11)	27.4	
		27.9	(10)
28.8	(10,12)	29.0	
30.1	(10,12)	29.9	
31.6	(12)		
32.5	(13)		
33.4	(11,13)		
34.2	(11)		

these breakup states, and it was speculated that these terminating states possessed a spin of  $J=14$ . These states observed in the high energy measurements of Murgatroyd *et al.* [16] are also seen the present measurements, and the angular correlation measurements demonstrate that the highest spin state observed is  $J=12$ . Thus, we can conclude that the re-

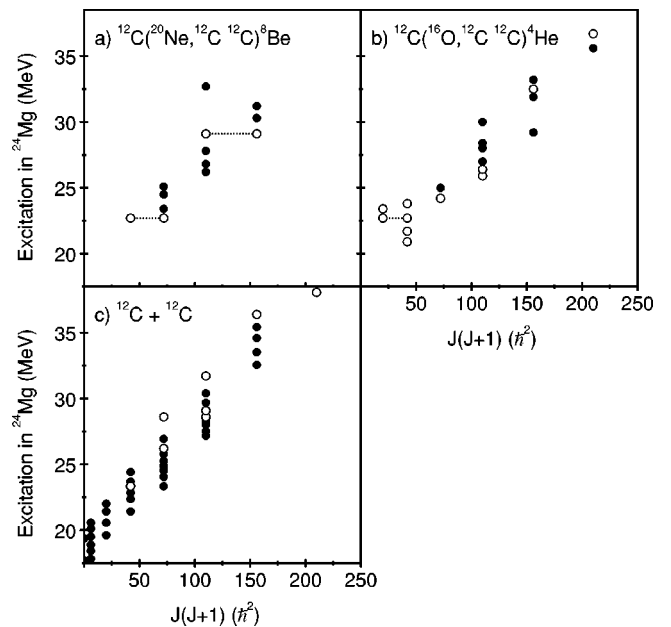


FIG. 8. The energy-spin systematics of resonances observed in the reactions (a)  $^{12}\text{C}(^{20}\text{Ne}, ^{12}\text{C}^{12}\text{C})$ , (b)  $^{12}\text{C}(^{16}\text{O}, ^{12}\text{C}^{12}\text{C})$ , and (c)  $^{12}\text{C}+^{12}\text{C}$ . The open circles correspond uncertain spin assignments. The results of a linear fit to the points is shown in Table V.

TABLE VI. The intercepts and gradients of the linear fits to the data in Fig. 8.

Reaction	Slope $\hbar^2/2I$ (KeV)	Intercept Bandhead (MeV)
$^{12}\text{C}(^{20}\text{Ne}, ^{12}\text{C } ^{12}\text{C})$	$75.8 \pm 1.5$	$19.13 \pm 0.16$
$^{12}\text{C}(^{16}\text{O}, ^{12}\text{C } ^{12}\text{C})$	$76.0 \pm 0.8$	$19.65 \pm 0.09$
$^{12}\text{C} + ^{12}\text{C}$ resonances	$101.3 \pm 0.3$	$18.46 \pm 0.04$

ported termination actually occurs at  $J=12$  and not  $J=14$ . On the other hand,  $J=14$  states are observed in the  $^{12}\text{C}(^{16}\text{O}, ^{12}\text{C } ^{12}\text{C})$  reaction in this region.

These observations may be explained by two possible scenarios. The first possibility is that the states observed in the  $^{12}\text{C} + ^{20}\text{Ne}$  measurement are confined entirely within the  $sd$ -shell (which would give  $J_{max}=12$  for the fully aligned configuration), and that the  $J=14$  states arise from a different  $^{24}\text{Mg}$  configuration within the  $fp$  shell. Alternatively, the states observed in the  $^{12}\text{C} + ^{20}\text{Ne}$  reaction correspond to a  $4p-4h$  excitation to the  $fp$  shell, which would result in  $J_{max}=20$  for the fully aligned  $sd$  and  $fp$ -shell nucleons, and that the transfer reaction only populates  $J_{max}=12$  states corresponding to the transfer of the  $\alpha$  particle into the orbits in the  $f_{7/2}$  orbit.

The fact that in the measurement of the  $^{12}\text{C}(^{16}\text{O}, ^{12}\text{C} + ^{12}\text{C})$  reaction the  $J=14$  resonances follow the continuation of the lower spin resonances on a  $J(J+1)$  trajectory (Fig. 8), does suggest that they are linked via a common structure, suggesting that the configuration is  $(sd)^4(fp)^4$ .

Thus, the present data suggest that the majority of the  $^{12}\text{C} + ^{12}\text{C}$  breakup states are associated with a configuration

built on a  $^{20}\text{Ne}$  core with a  $4p-4h$  excitation to the  $N=3$  shell. This association would consequently imply a connection with the shape isomeric  $\alpha$ - $^{16}\text{O}$ - $\alpha$  structure found in the Nilsson-Strutinsky [8], Hartree-Fock [9], and alpha cluster model [10] calculations, and supports the speculations originally made by Bennett *et al.* [19].

## V. CONCLUSIONS

The  $^{12}\text{C}(^{20}\text{Ne}, ^{12}\text{C } ^{12}\text{C})^8\text{Be}$  and  $^{12}\text{C}(^{20}\text{Ne}, ^8\text{Be } ^{16}\text{O})^8\text{Be}$  reactions have been studied, and the results indicate that specific states are populated in the excitation energy region 20 to 33 MeV that decay either by  $^{12}\text{C}$  or  $^8\text{Be}$  emission. The measurement of the angular distributions of the decay products suggests that the spins of the states lie between 6 and  $12\hbar$ . The levels observed in these decay channels appear to correspond in terms of both excitation energy and spins with those populated in the  $^{12}\text{C}(^{16}\text{O}, ^{12}\text{C } ^{12}\text{C})$  reaction. The observation that the states are much more strongly populated in the  $\alpha$ -transfer reaction [11] supports the notion that they are associated with a  $4p-4h$   $^{24}\text{Mg}$  excitation, based upon a  $^{20}\text{Ne}_{g.s.}$  core. This conclusion would further suggest that these states may be linked with the decay of a prolate,  $\alpha$ - $^{16}\text{O}$ - $\alpha$ ,  $^{24}\text{Mg}$  shape isomer.

## ACKNOWLEDGMENTS

The authors would like to acknowledge the financial support of the U.K. Engineering and Physical Sciences Research Council. The work of the Physics Division, Argonne National Laboratory is supported by the U.S. Department of Energy, Nuclear Physics Division, under Contract No. W-31-109-Eng-38.

- 
- [1] D. Robson, Nucl. Phys. **A204**, 523 (1973).  
[2] E. F. da Silveria, Proceedings of the 14th Winter Meeting on Nuclear Physics, Bormio, 1976 (unpublished).  
[3] W. D. M. Rae and R. K. Bhowmik, Nucl. Phys. **A420**, 320 (1984).  
[4] B. R. Fulton, S. J. Bennett, M. Freer, J. T. Murgatroyd, G. J. Gyapong, N. S. Jarvis, C. D. Jones, D. L. Watson, J. D. Brown, W. D. M. Rae, A. E. Smith, and J. S. Lilley, Phys. Lett. B **267**, 325 (1991).  
[5] N. Curtis *et al.*, Phys. Rev. C **51**, 1554 (1995).  
[6] M. Freer, N. M. Clarke, B. R. Fulton, J. T. Murgatroyd, A. St. J. Murphy, S. P. G. Chappell, R. L. Cowin, G. Dillon, D. L. Watson, W. N. Catford, N. Curtis, M. Shawcross, and V. F. E. Pucknell, Phys. Rev. C **57**, 1277 (1998).  
[7] K. A. Erb and D. A. Bromley, in *Treatise on Heavy-Ion Science*, edited by D. A. Bromley (Plenum, New York, 1984), Chap. 3, Vol. 3, pp. 201–310.  
[8] G. Leander and S. E. Larsson, Nucl. Phys. **A239**, 93 (1975).  
[9] H. Flocard, P. H. Heenen, S. J. Krieger, and M. S. Weiss, Prog. Theor. Phys. **72**, 1000 (1984).  
[10] S. Marsh and W. D. M. Rae, Phys. Lett. B **180**, 185 (1986).  
[11] M. Freer and A. C. Merchant, J. Phys. G **23**, 383 (1997).  
[12] B. R. Fulton, S. J. Bennett, J. T. Murgatroyd, N. S. Jarvis, D. L. Watson, W. D. M. Rae, Y. Chan, D. DiGregorio, J. Scarpaci, J. Suro Perez, and R. G. Stokstad, J. Phys. G **20**, 151 (1994).  
[13] J. T. Murgatroyd, J. S. Pople, N. M. Clarke, B. R. Fulton, M. J. Leddy, W. N. Catford, S. P. Fox, G. J. Gyapong, C. D. Jones, D. L. Watson, W. D. M. Rae, Y. Chan, R. G. Stokstad, and S. J. Bennett, Phys. Rev. C **58**, 1569 (1998).  
[14] N. Curtis *et al.*, Nucl. Instrum. Methods Phys. Res. A **351**, 359 (1994).  
[15] M. Freer, Nucl. Instrum. Methods Phys. Res. A **383**, 463 (1996).  
[16] J. T. Murgatroyd, S. J. Bennett, N. M. Clarke, B. R. Fulton, G. J. Gyapong, C. D. Jones, D. L. Watson, T. M. Cormier, H. Dejbakhsh, A. Sznto de Toledo, and N. Carlin, Nucl. Phys. **A587**, 367 (1995).  
[17] J. T. Murgatroyd, Ph.D. thesis, University of Birmingham, 1992.  
[18] D. M. Brink, Phys. Lett. **40B**, 37 (1972).  
[19] S. J. Bennett, M. Freer, B. R. Fulton, J. T. Murgatroyd, P. J. Woods, S. C. Allcock, W. D. M. Rae, A. E. Smith, J. S. Lilley, and R. R. Betts, Nucl. Phys. **A534**, 445 (1991).